On simplifying 'incremental remap'-based transport schemes

Peter H. Lauritzen[a,*], Christoph Erath[b], Rashmi Mittal[c]

[a]*Climate and Global Dynamics Division, National Center for Atmospheric Research, P.O. Box 3000, Boulder, CO 80307, USA*
[b]*The Computational & Information Systems Laboratory, National Center for Atmospheric Research, P.O. Box 3000, Boulder, CO 80307, USA*
[c]*Mesoscale and Microscale Meteorology Division, National Center for Atmospheric Research, P.O. Box 3000, Boulder, CO 80307-3000*

Abstract

The flux-form incremental remapping transport scheme introduced by Dukowicz and Baumgardner [1] converts the transport problem into a remapping problem. This involves identifying overlap areas between quadrilateral flux-areas and regular square grid cells which is non-trivial and leads to some algorithm complexity. In the simpler *swept area* approach (originally introduced by Hirt et al. [2]) the search for overlap areas is eliminated even if the flux-areas overlap several regular grid cells. The resulting *simplified* scheme leads to a much simpler and robust algorithm.

We show that for sufficiently small Courant numbers (approximately CFL≤1/2) the simplified (or swept area) scheme can be more accurate than the original incremental remapping scheme. This is demonstrated through a Von Neumann stability analysis, an error analysis and in idealized transport test cases on the sphere using the 'incremental remapping'-based scheme called FF-CSLAM (Flux-Form version of the Conservative Semi-Lagrangian Multi-tracer scheme) on the cubed-sphere.

Keywords: Conservative Transport, Cubed-sphere, Error Analysis, Finite-Volume, Flux-Form Semi-Lagrangian, Von Neumann Stability Analysis, Remapping, Multi-Tracer Transport

1. Introduction

Consider the flux-form continuity equation for some inert and passive mass variable ψ (for example, fluid density ρ or tracer density $\rho\, q$, where q is a mixing ratio)

$$\frac{\partial \psi}{\partial t} + \nabla \cdot (\psi\, \vec{v}) = 0, \tag{1}$$

where $\vec{v} = (u, v)$ is the velocity vector. Following [1], the 2D Cartesian discretization of the integral form of (1) for a particular grid cell A can be written as

$$\left(\overline{\psi}^{n+1} - \overline{\psi}^{n}\right) |A| - (F_W + F_S + F_E + F_N) = 0, \tag{2}$$

*Corresponding author. Tel.: +1 303 497 1316; fax: +1 303 497 1324.
Email address: pel@ucar.edu (Peter H. Lauritzen)
URL: http://www.cgd.ucar.edu/cms/pel/ (Peter H. Lauritzen)
[1]The National Center for Atmospheric Research is sponsored by the National Science Foundation.

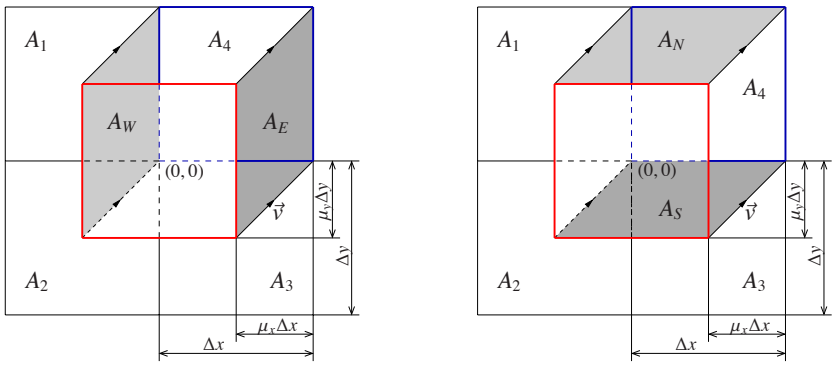

(a) West and east cell edge.

(b) North and south cell edge.

Figure 1: Graphical illustration of the rigorous and simplified schemes for a constant traverse flow ($u = v$). In both subfigures, $A_1 \ldots A_4$ denote the Eulerian grid cells. The domains A_W, A_E A_N, and A_S (gray) represent the flux-areas for the respective cell edges. See text for more details.

where $\overline{(\cdot)}$ refers to the cell-averaged value, n the time-level index, $|A| = \Delta x\,\Delta y$ is the area of the grid cell, F_W is the flux of mass into the cell through its West cell edge (here we use standard compass point notation), and similarly for the East, North and South cell edges. In the incremental remapping approach, the flux is approximated through integration of the reconstruction function $\psi^n(x, y)$ over the area 'swept' through the cell edge during a time-step Δt; these areas are referred to as the *flux-areas* A_W, A_E, A_N and A_S for the respective cell edges as shown on Fig. 1. For a recent review of 'remap-type' tracer transport schemes see the book chapter [3].

The incremental remapping scheme and simplified schemes are described with the aid of Fig. 1. The flux-areas are approximated with quadrilaterals with the end points of the cell edges as vertices as well as their upstream translated counterparts (shaded areas on Fig. 1). We assume that trajectories do not cross. In the incremental remapping algorithm presented in [1] the flux of mass through the West cell edge is given in terms of integrals over overlap areas between A_W and the regular grid cells A_1 and A_2 such that

$$F_W = \int_{A_1 \cap A_W} \psi_1^n(x, y)\, dx\, dy + \int_{A_2 \cap A_W} \psi_2^n(x, y)\, dx\, dy, \tag{3}$$

where $\psi_j^n(x, y)$ is the reconstruction function in cell j (see [1] for details). Similarly for the East, North, and South cell edges. Note that $F_W, F_S \geq 0$ and $F_E, F_N \leq 0$ in Fig. 1.

For the West cell edge and simply-connected flux-area A_W, the simplified scheme only uses one sub-grid-cell reconstruction function (either the one immediately to the East or West of the cell edge) for the entire flux integral, even if the flux-area spans more regular grid cells. This approach, equivalent to the donor cell option in [2], is widely used in the literature and often referred to as *swept area* remapping [e.g. 4, 5, 6]. The reconstruction function used is the one 'upstream'. That is, for the West edge the reconstruction function $\psi_1^n(x, y)$ is used if $|A_1 \cap A_W| \geq 0$

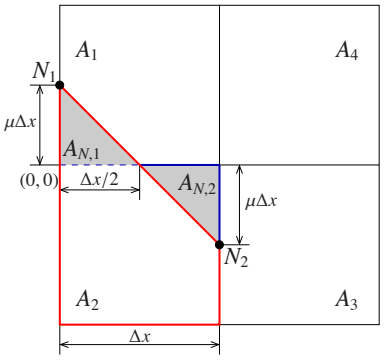

(a) 'Anti clockwise' hourglass movement of the North edge.

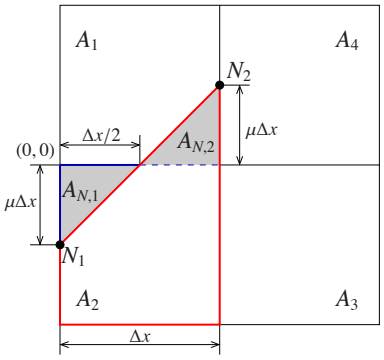

(b) 'Clockwise' hourglass movement of the North edge.

Figure 2: Hourglass velocity movement: In Subfigure (a) point N_1 moves with $\vec{v} = (0, -v)$, $v > 0$ whereas N_2 with $\vec{v} = (0, v)$. In Subfigure (b) the movement is vice versa. In both figures the other nodes do not move. The fluxes through the East, South and West edges are 0 in both cases.

else $\psi_4^n(x, y)$. For the situation depicted on Fig. 1 the simplified fluxes are

$$F_W^{simple} = \int_{A_W} \psi_1^n(x, y)\, dx\, dy, \qquad F_E^{simple} = -\int_{A_E} \psi_4^n(x, y)\, dx\, dy, \tag{4}$$

$$F_N^{simple} = -\int_{A_N} \psi_4^n(x, y)\, dx\, dy, \qquad F_S^{simple} = \int_{A_S} \psi_3^n(x, y)\, dx\, dy. \tag{5}$$

Note that for CFL≤1 and flow parallel to either of the coordinate directions, the rigorous and simplified schemes are identical

$$F_T^{simple} = F_T, \qquad \text{for } \vec{v} = (u, 0) \text{ or } \vec{v} = (0, v), \tag{6}$$

where $T \in \{N, S, E, W\}$. Hence the rigorous and simplified schemes differ the most when the flow is traverse to the grid lines ($\vec{v} = (u, u) = (v, v)$).

For flux areas that are not simply-connected (i.e. where the flow direction normal to the cell face changes resulting in overlap areas on either side of the cell edge as illustrated on Fig. 2), there are basically two approaches for computing the flux within the simplified scheme methodology. We use the situation depicted on Fig. 2(a) to explain the schemes.

The flux-area A_N is split into two triangles $A_{N,1}$ and $A_{N,2}$, one on each side of the North flux-face. In this case $A_{N,1}$ is located to the North and $A_{N,2}$ to the South of the flux edge, respectively. One can either choose to use the same reconstruction function (determined by the largest overlap area) to integrate over $A_{N,1}$ and $A_{N,2}$

$$F_N^{simple} = \begin{cases} \int_{A_{N,1}} \psi_1^n(x, y)\, dx\, dy - \int_{A_{N,2}} \psi_1^n(x, y)\, dx\, dy & \text{if } |A_{N,1}| > |A_{N,2}|, \\ \int_{A_{N,1}} \psi_2^n(x, y)\, dx\, dy - \int_{A_{N,2}} \psi_2^n(x, y)\, dx\, dy & \text{else,} \end{cases} \tag{7}$$

or one can choose to use the reconstruction function immediately to the North and South of the flux edge to integrate over $A_{N,1}$ and $A_{N,2}$, respectively,

$$F_N^{simple} = \int_{A_{N,1}} \psi_1^n(x, y)\, dx\, dy - \int_{A_{N,2}} \psi_2^n(x, y)\, dx\, dy. \tag{8}$$

Similarly for the East, West and South faces. As for the simply connected flux-integrals, even if the triangular area $A_{N,1}$ span more Eulerian cells only one reconstruction function is used to integrate over $A_{N,1}$ (similarly for $A_{N,2}$). For the flow situations depicted on Fig. 2 the simplified scheme (8) is equivalent to the rigorous scheme since $A_{N,1}$ and $A_{N,2}$ do not span more than one Eulerian cell.

First a Von Neumann stability and error analysis of the rigorous (original incremental remapping) and simplified schemes is presented for a traverse flow for which the flux-areas are simply-connected (quadrilaterals). An error analysis for the 'hourglass' flow is presented as well to investigate the accuracy when the flux-areas are not simply connected. Both of these flow situations appear frequently in practical simulations. Thereafter results for idealized transport test cases on sphere, using a flux-form version of the CSLAM scheme [7] on the cubed-sphere (referred to as FF-CSLAM [8]), based on rigorous and simplified fluxes are presented.

2. Theoretical analysis

2.1. Von Neumann stability analysis - traverse flow

We closely follow the Von Neumann analysis of [9], that is, assume a constant velocity $\vec{v} = (u, v)$ with $u = v$ (traverse flow which is the most challenging case [9]), and $\Delta x = \Delta y$. Assume a solution in the form

$$\psi^n(x, y) := \psi^0 \Gamma^n e^{\imath(k_x x + k_y y)},$$

where $\imath$ is the imaginary unit, ψ^0 the initial amplitude, $k_x = 2\pi/L_x$ and $k_y = 2\pi/L_y$ are the wavenumbers in each coordinate direction (L_x and L_y are the corresponding wave lengths), respectively, and Γ is the complex amplification factor that can be written as

$$\Gamma = |\Gamma| e^{-\imath\omega^* \Delta t}, \tag{9}$$

where ω^* is the numerical frequency. We define the relative frequency $R := \omega^*/\omega$ in terms of the exact frequency

$$\omega = \mu \left(k_x \Delta x + k_y \Delta y \right), \tag{10}$$

where $\mu := \mu_x = \mu_y = u\,\Delta t/\Delta x = v\,\Delta t/\Delta y$ is the dimensionless displacement parameter that is identical in each coordinate direction for traverse flow and equidistant grid-spacing. The scheme is unstable for $|\Gamma| > 1$. For simplicity we assume 'symmetric' waves, i.e. $L_x = L_y$.

As in [9] the von Neumann stability analysis is performed for three reconstruction functions: Piecewise Constant Method (PCM) where $\psi_j^n(x, y)$ is a constant function in each grid cell, Piecewise Linear Method (PLM) where $\psi_j^n(x, y)$ is a 2D bilinear function as used in [1], and Piecewise Parabolic Method (PPM) where $\psi_j^n(x, y)$ is a fully 2D biparabolic reconstruction function with cross-terms (see [7] for details). Fig. 3 depicts the squared modulus of the amplification factor $|\Gamma|^2$ and relative frequency R for the rigorous incremental remapping and simplified scheme.

Considering first $|\Gamma|^2$ we note that the simplified scheme based on any of the reconstruction methods is less damping than the rigorous scheme for $\mu \leq 1/2$. In fact, the simplified scheme based on PCM or PLM is exact ($|\Gamma|^2 = 1$ and $R = 1$) for $\mu = 1/2$ contrary to the rigorous scheme that is most damping for $\mu = 1/2$. When μ exceeds half the simplified scheme based on PCM and PLM becomes unstable. When using PPM the simplified scheme starts damping more than the rigorous scheme for $\mu > 1/2$ and becomes unstable for the shortest wavelength for $\mu > 3/4$ (for wavelengths longer than approximately $L_x = L_y = 4$ the simplified scheme is stable for

Courant numbers exceeding one). The simplified scheme most likely becomes unstable because the region of 'extrapolation' (overlap between flux-area and non-adjacent upstream grid cell, e.g., $A_2 \cap A_W$ for A_W) becomes too large compared to the flux-overlap-area adjacent and upstream to the cell edge (e.g., $A_1 \cap A_W$). Similar observations are made for the relative frequency R.

2.2. Error analysis - traverse flow

In the error analysis we make the same assumptions as for the Von Neumann stability analysis. For simplicity we assume PCM and analyze the situation depicted on Fig. 1. Let $\psi^n(x,y) = e^{\imath(k_x x + k_y y)}$ denote the exact solution so that the exact mean flux over an area A_j is

$$\overline{\psi}_j = \frac{1}{|A_j|}\int_{A_j} \psi^n(x,y)\,dx\,dy,$$

which represents the approximation on the Eulerian grid A_j, $j = 1\ldots4$. The numerical flux, which enters the West cell edge of A_4, for the rigorous and simplified scheme are

$$F_W = |A_1 \cap A_W|\,\overline{\psi}_1 + |A_2 \cap A_W|\,\overline{\psi}_2 \quad \text{and} \quad F_W^{simple} = |A_W|\,\overline{\psi}_1,$$

respectively. The exact flux on the West cell edge is

$$F_W^{exact} = \int_{A_W} \psi^n(x,y)\,dx\,dy.$$

With the parameter $\mu = u\Delta t/\Delta x$ we can write $|A_1 \cap A_W| = (\mu - \mu^2/2)\Delta x^2$ and $|A_2 \cap A_W| = (\mu^2/2)\Delta x^2$. Note that we assume $\Delta x = \Delta y$ and $u = v$. For the other sides the approximation is done similarly according to Fig. 1. With this notation, the errors for the rigorous scheme, $\epsilon_T := F_T^{exact} - F_T$ for $T \in \{W, E, N, S\}$, are given by

$$\begin{aligned}
\epsilon_W &= \imath\,\Delta x^3 \frac{1}{2} k_x \mu(1-\mu) + O(\Delta x^4) \quad \& \quad \epsilon_E = -\imath\,\Delta x^3 \frac{1}{2} k_x \mu(1-\mu) + O(\Delta x^4),\\
\epsilon_S &= \imath\,\Delta x^3 \frac{1}{2} k_y \mu(1-\mu) + O(\Delta x^4) \quad \& \quad \epsilon_N = -\imath\,\Delta x^3 \frac{1}{2} k_y \mu(1-\mu) + O(\Delta x^4).
\end{aligned} \tag{11}$$

The above is computed by evaluating the integrals with respect to the origin $(0,0)$ according to Fig. 1 and then writing the errors in a Taylor Series expansion. Similarly for the simplified scheme the errors, $\epsilon_T^{simple} := F_T^{exact} - F_T^{simple}$, are given by

$$\begin{aligned}
\epsilon_W^{simple} &= \imath\,\Delta x^3 \frac{1}{2} \mu(k_x - \mu(k_x + k_y)) + O(\Delta x^4) \quad \& \quad \epsilon_E^{simple} = -\imath\,\Delta x^3 \frac{1}{2} \mu(k_x - \mu(k_x + k_y)) + O(\Delta x^4),\\
\epsilon_S^{simple} &= \imath\,\Delta x^3 \frac{1}{2} \mu(k_y - \mu(k_x + k_y)) + O(\Delta x^4) \quad \& \quad \epsilon_N^{simple} = -\imath\,\Delta x^3 \frac{1}{2} \mu(k_y - \mu(k_x + k_y)) + O(\Delta x^4).
\end{aligned} \tag{12}$$

Note that $\epsilon_{W,E}$ and $\epsilon_{N,S}$ in (11) are independent of k_y and k_x, respectively, since the corresponding wave part is parallel to the sides.

The errors $\epsilon_{W,E}$ and $\epsilon_{W,E}^{simple}$ differ in the terms of

$$k_x(1-\mu) \quad \text{and} \quad k_x - \mu(k_x + k_y),$$

so if

$$0 < \mu < \frac{2k_x}{2k_x + k_y}$$

then the simplified scheme using only one reconstruction function instead of two is more accurate. Note that $k_x, k_y > 0$. Similarly for the errors $\epsilon_{S,N}$ and $\epsilon_{S,N}^{simple}$ where we get

$$0 < \mu < \frac{2k_y}{2k_y + k_x}.$$

For $k_x = k_y$ the errors ϵ_T and ϵ_T^{simple} for $T \in \{W, E, N, S\}$ only differ in one factor, namely $1-\mu$ versus $1 - 2\mu$. That means, the absolute error of the simplified scheme fluxes is indeed better at least for $0 < \mu < 2/3$, which is in the stability range $\mu \in (0, 1/2)$. In other words the absolute value of ϵ_T^{simple} is $(1 - \mu)/(1 - 2\mu)$-times better than ϵ_T.

2.3. Error analysis - 'hourglass' flow

The Von Neumann stability and error analysis assumed a traverse flow for which the flux-areas are simply-connected quadrilaterals. Here we analyze a situation, that appears frequently in practial (non-idealized) simulations, in which the flux-area is non-simple using the 'hourglass' velocity field for the North flux edge. That is, the West node N_1 for the Northern flux edge moves Southward with $\vec{v} = (0, -v)$, $v > 0$ and the East node N_2 moves in the opposite direction (Northward) at the same rate $\vec{v} = (0, v)$ (Fig. 2(a)) or vice versa (Fig. 2(b)). The flux-area is non-simple and can be divided into a triangle North of the flux edge ($A_{N,1}$) and South of the flux edge ($A_{N,2}$). All other nodes for the cell are stationary so there is no flux through the East, West and South cell edges.

For the situation depicted on Fig. 2(a) the exact flux is

$$F_N^{exact} = \int_{A_{N,1}} \psi(x, y)\, dx\, dy - \int_{A_{N,2}} \psi(x, y)\, dx\, dy.$$

The numerical flux for the simplified scheme using two reconstruction functions (which in this case is identical to the rigorous scheme since $|A_{N,1} \cap A_1| = |A_{N,1}|$ and $|A_{N,2} \cap A_2| = |A_{N,2}|$) and simplified scheme based on one reconstruction function for the integral over $A_{N,1} \cup A_{N,2}$ are

$$F_N = |A_{N,1}|\,\overline{\psi}_1 - |A_{N,2}|\,\overline{\psi}_2 = |A_{N,1}|\,(\overline{\psi}_1 - \overline{\psi}_2)$$

(note that $|A_{N,1}| = |A_{N,2}|$) and

$$\begin{aligned} F_N^{simple} &= |A_{N,1}|\,\overline{\psi}_1 - |A_{N,2}|\,\overline{\psi}_1 = 0 \\ &= |A_{N,1}|\,\overline{\psi}_2 - |A_{N,2}|\,\overline{\psi}_2 = 0, \end{aligned}$$

respectively. Using the same techniques as used for the error analysis for the traverse flow presented above and the point of origin as in Fig. 2(a), leads to

$$\epsilon_{N,H} = \imath\, \Delta x^3 \frac{1}{12} \mu (k_y(2\mu - 3) - 2k_x) + O(\Delta x^4) \quad \text{and} \quad \epsilon_{N,H}^{simple} = \imath\, \Delta x^3 \frac{1}{6} \mu (k_y \mu - k_x) + O(\Delta x^4). \tag{13}$$

The errors $\epsilon_{N,H}$ and $\epsilon_{N,H}^{simple}$ differ in the terms of

$$k_y\left(\mu - \frac{3}{2}\right) - k_x \quad \text{and} \quad k_y\mu - k_x,$$

so if

$$\mu < \frac{3}{4} + \frac{k_x}{k_y}, \tag{14}$$

then the simplified scheme using only one reconstruction function instead of two is more accurate. The condition (14) is always met in practice since $k_x, k_y > 0$ and $0 \leq \mu \ll 1$.

If we change the sign of v so that node N_1 moves with $v > 0$ whereas N_2 with $-v$ (see Fig. 2b) and perform the same analysis, the corresponding errors are

$$\epsilon_{N,H} = \imath\,\Delta x^3 \frac{1}{12}\mu(k_y(2\mu - 3) + 2k_x) + O(\Delta x^4) \quad \text{and} \quad \epsilon_{N,H}^{simple} = \imath\,\Delta x^3 \frac{1}{6}\mu(k_y\mu + k_x) + O(\Delta x^4). \tag{15}$$

Now the errors differ by

$$k_y\left(\mu - \frac{3}{2}\right) + k_x \quad \text{and} \quad k_y\mu + k_x.$$

so the simplified scheme using only one reconstruction function is more accurate than the simplified scheme using two reconstruction functions for the flux-integral over A_N only if

$$\mu < \frac{3}{4} - \frac{k_x}{k_y}.$$

For symmetric waves ($k_x = k_y$) the simplified scheme is always more accurate for the 'anti-clockwise' flow (Fig. 2(a)) whereas for the 'clockwise' flow (Fig. 2(b)) the rigorous scheme is always more accurate.

3. Results

To evaluate if the findings for the linear analysis also hold in more complicated settings, we use the global transport scheme FF-CSLAM on the cubed-sphere grid. The FF-CSLAM scheme is based on the incremental remapping algorithm but extended to the sphere and third-order accuracy. Also, instead of using Gaussian quadrature the overlap integrals are converted to line-integrals on the gnomonic projection using the Divergence theorem which provides a rigorous treatment of the metric terms [12]. Since the cubed-sphere discretization is based on quadrilaterals in computational space, the simplified FF-CSLAM scheme is implemented exactly as outlined in Cartesian geometry. Each of the cubed-sphere panels is partitioned into N^2 cells, and the equivalent resolution with respect to the regular latitude-longitude sphere at the equator is approximately $90^\circ/N$. For all simulations we use $N = 60$ corresponding to approximately 1.5° resolution. We solve the coupled system of continuity equations for air density ρ and tracer density ρq as described in [11]. Initial condition for ρ is one everywhere and q is non-constant as described below for the particular test cases. The coupling between the continuity equation for ρ

Table 1: Standard error norms for q for the translational (solid-body), moving vortices [10], and highly deformational [11] ('boomerang') test cases for different configurations of the third-order FF-CSLAM scheme. Maximum CFL number (the longest distance traveled by a parcel in units of the grid-spacing) of the two coordinate directions locally on each cubed-sphere panel is approximately 0.42, 0.53, and 0.53 for each of the three test cases, respectively.

Scheme	Experiment	ℓ_1	ℓ_2	ℓ_∞	$\phi_{\max}$	$\phi_{\min}$
rigorous	solid-body	0.0013	0.0063	0.0104	–0.0025	–0.0077
simplified	solid-body	0.0012	0.0061	0.0102	–0.0026	–0.0077
rigorous	moving vortices	0.0018	0.0064	0.0332	0.0000	0.0000
simplified	moving vortices	0.0016	0.0060	0.0309	0.0000	0.0000
rigorous	'boomerang'	0.0565	0.1150	0.1548	–0.1403	–0.0573
simplified	'boomerang'	0.0551	0.1126	0.1503	–0.1386	–0.0571

and $\rho\, q$ in FF-CSLAM is described in Appendix A of [8]. All error norms are based on mixing ratio q. Below we do not distinguish between the two versions of the simplified scheme for non-simple flux-areas since the results were indistinguishable in terms of standard error norms most likely since the non-simple flux areas are very rare for the idealized test cases considered here.

First we use the standard solid-body test case [13] and the exact same setup as [14], that is, rotation angle 45° (predominantly traverse flow on the Equatorial cubed-sphere panels), one revolution completed in 576 time-steps and cosine hill initial condition for q (with amplitude 1000 and radius 1/3). Standard error norms (see, e.g., Appendix C in [11]) for the rigorous and simplified schemes are given in Table 1. The simplified scheme is slightly more accurate than the rigorous scheme as expected from the Von Neumann stability analysis for traverse flows. Similar results are obtained with the moving vortices test case [10] (Δt is chosen such that one revolution is completed in 576 time-steps as in [14]).

To challenge the scheme more we use the recently developed strongly deformational test case on the sphere [11] (their Case-4). The time-step is chosen such that the simulation is completed in 1200 time-steps and cosine hills initial condition is used. Again, the findings are very similar to the solid-body transport case even though the flow is strongly deformational.

4. Conclusions

In this paper we have demonstrated that the incremental remapping algorithm for small Courant numbers (approximately CFL<1/2) can be simplified significantly with minimal changes in accuracy. The simplification is only to use the reconstruction function in the cell immediately upstream to a cell face for the entire flux computation and, hence, no search for overlap areas that is necessary for the original (rigorous) incremental remapping algorithm is needed. The simplified scheme (unlimited) is slightly more accurate in idealized test cases on the sphere using the 'incremental remapping'-type FF-CSLAM scheme on the cubed-sphere. Therefore a Von Neumann stability analysis and error analysis on the Cartesian plane with traverse as well as 'hourglass' flows were performed and those confirmed our findings.

Although the computational cost of the search algorithm in the rigorous incremental remapping scheme becomes marginal for an increased number of tracers, we believe that the simplified

scheme will render this flux-form semi-Lagrangian method more robust and computationally competitive even for a small number of tracers. For large Courant numbers, however, the rigorous scheme, e.g. FF-CSLAM, must be used.

Acknowledgements

The careful reviews by Dr. R.D.Nair (NCAR) and Dr. L.M. Harris (GFDL) are gratefully acknowledged. The authors were partially supported by the DOE BER Program under award DE-SC0001658. We thank two anonymous reviewers for their helpful comments and suggestions that have significantly improved this manuscript.

References

[1] J. K. Dukowicz, J. R. Baumgardner, Incremental remapping as a transport/advection algorithm, J. Comput. Phys. 160 (2000) 318–335.

[2] C. W. Hirt, A. A. Amsden, J. L. Cook, An arbitrary Lagrangian-Eulerian computing method for all flow speeds, J. Comput. Phys. 14 (3) (1974) 227 – 253.

[3] P. H. Lauritzen, P. A. Ullrich, R. D. Nair, Atmospheric transport schemes: Desirable properties and a semi-Lagrangian view on finite-volume discretizations, Vol. 80 of Lecture Notes in Computational Science and Engineering (Tutorials), Springer, 2011, Ch. 8, pp. 185–251.

[4] L. G. Margolin, M. Shashkov, Second-order sign-preserving conservative interpolation (remapping) on general grids, J. Comput. Phys. 184 (2003) 266–298.

[5] M. Kucharik, M. Shashkov, B. Wendroff, An efficient linearity-and-bound-preserving remapping method, J. Comput. Phys. 188 (2) (2003) 462 – 471.

[6] R. Loubère, M. J. Shashkov, A subcell remapping method on staggered polygonal grids for arbitrary-Lagrangian-Eulerian methods, J. Comput. Phys. 209 (1) (2005) 105 – 138.

[7] P. H. Lauritzen, R. D. Nair, P. A. Ullrich, A conservative semi-Lagrangian multi-tracer transport scheme (CSLAM) on the cubed-sphere grid, J. Comput. Phys. 229 (2010) 1401–1424.

[8] L. M. Harris, P. H. Lauritzen, R. Mittal, A flux-form version of the conservative semi-Lagrangian multi-tracer transport scheme (CSLAM) on the cubed sphere grid, J. Comput. Phys. 230 (4) (2010) 1215–1237.

[9] P. H. Lauritzen, A stability analysis of finite-volume advection schemes permitting long time steps, Mon. Wea. Rev. 135 (2007) 2658–2673.

[10] R. D. Nair, C. Jablonowski, Moving vortices on the sphere: A test case for horizontal advection problems, Mon. Wea. Rev. 136 (2008) 699–711.

[11] R. D. Nair, P. H. Lauritzen, A class of deformational flow test cases for linear transport problems on the sphere, J. Comput. Phys. 229 (2010) 8868–8887.

[12] P. A. Ullrich, P. H. Lauritzen, C. Jablonowski, Geometrically exact conservative remapping (GECoRe): Regular latitude-longitude and cubed-sphere grids., Mon. Wea. Rev. 137 (6) (2009) 1721–1741.

[13] D. L. Williamson, J. B. Drake, J. J. Hack, R. Jakob, P. N. Swarztrauber, A standard test set for numerical approximations to the shallow water equations in spherical geometry, J. Comput. Phys. 102 (1992) 211–224.

[14] W. M. Putman, S.-J. Lin, Finite-volume transport on various cubed-sphere grids, J. Comput. Phys. 227 (1) (2007) 55–78.

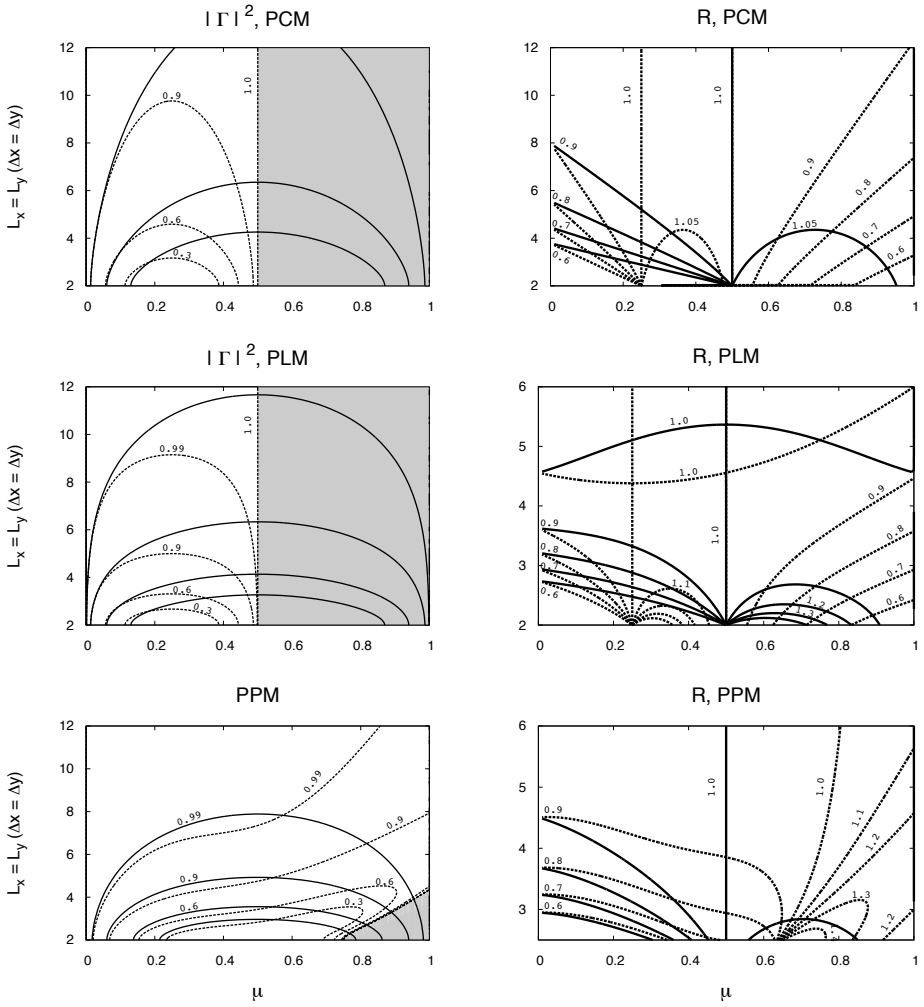

Figure 3: Squared modulus of the amplification $|\Gamma|^2$ (first column) and relative frequency R (second column) for the rigorous incremental remapping scheme (solid lines) and simplified scheme (dashed lines) as a function of the displacement parameter μ and wavelength L for traverse flow ($\mu = \mu_x = \mu_y$) and 'symmetric' waves ($L_x = L_y$). Contours are marked on the plots and the shaded areas mark where the simplified scheme is unstable ($|\Gamma|^2 \geq 1$). First, second, and third rows are for reconstruction functions based on the PCM, PLM, and PPM, respectively.